PHYSICAL REVIEW D VOLUME 48, NUMBER 10 15 NOVEMBER 1993

Resummation methods at finite temperature: The tadpole way

C. Glenn Boyd*
Enrico Fermi Institute, 5640 Ellis Avenue, Chicago, Illinois 60637

David E. Brahm†
California Institute of Technology, Mail code 452-48, Pasadena, California 91125

Stephen D. H. Hsu‡
Lyman Laboratory of Physics, Harvard University, Cambridge, Massachusetts 02138
(Received 19 April 1993)

We examine several resummation methods for computing higher order corrections to the finite temperature effective potential, in the context of a scalar ϕ^4 theory. We show by explicit calculation to four loops that dressing the propagator, not the vertex, of the one-loop tadpole correctly counts "daisy" and "superdaisy" diagrams.

PACS number(s): 11.15.Ex, 05.70.Fh, 12.15.Ji, 98.80.Cq

I. INTRODUCTION: RESUMMATION OF DAISIES

Recent interest in the electroweak phase transition (EWPT) has led to attempts to improve the finite temperature effective potential by resummation of leading infrared divergent graphs [1–9]. There is some controversy over the correct resummation procedure, particularly how "daisy" and "superdaisy" [10] graphs are accounted for by dressing the propagator and/or vertex in one-loop tadpole graphs. Espinosa, Quiros, and Zwirner [5] advocate a method which at the tadpole level amounts to dressing both propagator and vertex ("full dressing"), while we claim [4] that dressing the tadpole's propagator alone ("partial dressing") accurately counts higher-loop graphs. In this paper we show by explicit calculation to four loops in a scalar theory that partial dressing reproduces the correct combinatorics, while full dressing overcounts an infinite set of diagrams.

We also discuss other methods in the literature. Arnold and Espinosa [8] have reported that resummation corrections make the EWPT more strongly first order. We verify that their counting scheme, applied to the scalar theory, is equivalent to partial dressing; and unlike either superdaisy resummation scheme, it handles overlapping momenta correctly.

In Sec. II, after introducing our notation, we compare full to partial dressing (graphically and algebraically) in a region of parameter space where trilinear couplings are small, and calculate the higher-loop diagrams explicitly. Trilinear couplings are considered in more detail in Sec. III, some earlier approximations are eliminated, and questions of overlapping momenta are addressed. Our result for the effective potential is then presented. In Sec. IV we examine the Cornwall, Jackiw, and Tomboulis procedure [11, 12], the Arnold-Espinosa loop expansion [8], and the two-point method of Buchmuller *et al.* [13], and suggest a hybrid method with the best features of the others. We summarize our findings in Sec. V.

II. VACUUM OR TADPOLE?

Consider a real scalar field theory with tree-level potential $V_0 = \frac{\lambda}{4}\phi^4 - \frac{\mu^2}{2}\phi^2$. The effective potential is given by minus the sum of all vacuum-to-vacuum graphs; the one-loop contribution is

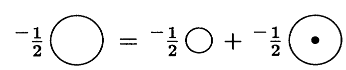

$$= \left(\frac{-\pi^2 T^4}{90} + \frac{T^2 m^2}{24} + \cdots\right) - \frac{T m^3}{12\pi}. \quad (1)$$

We have separated the $n \neq 0$ modes (small loop) and the $n=0$ mode (dotted loop), displayed symmetry factors explicitly, and kept only terms $O(T)$ or higher. Here $m^2 = V_0'' = 3\lambda\phi^2 - \mu^2$, and n is the Matsubara frequency index. Over regions of ϕ where $m \to 0$, infrared divergences appearing in the zero-mode contribution must be compensated by including higher-loop "daisy" and "superdaisy" diagrams [10], which give the scalar an effective "plasma mass."

An alternative approach [1, 14] is to calculate the derivative $V'(\phi)$, given by the sum of all tadpole graphs, and then integrate with respect to ϕ. The tadpoles are given correctly, including symmetry factors, by attaching a ($p=0$ truncated) external line to each part of each vacuum graph, e.g.,

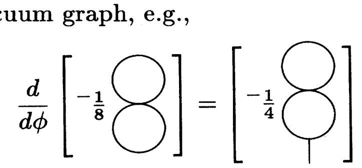

(2)

---

*Electronic address: boyd@rabi.uchicago.edu
†Electronic address: brahm@theory3.caltech.edu
‡Electronic address: hsu@hsunext.harvard.edu

0556-2821/93/48(10)/4963(11)/$06.00

When we discuss a method from the literature which uses vacuum graphs (e.g., [5, 6, 8, 11, 12]), we will usually convert it to tadpoles (take $d/d\phi$) to facilitate a comparison.

While hard thermal loops (daisies) can be included by shifting the mass with a temperature-dependent term in either vacuum or tadpole graphs, higher order corrections (superdaisies) require a field-dependent mass shift which gives different results if inserted into the vacuum rather than tadpole diagrams. There has been confusion in the literature over which method properly incorporates the important higher-loop superdaisy diagrams. It is known, for example, that a simple shift $m^2 \to m^2 + \Pi(\phi, T)$ in the one-loop contribution to the effective potential Eq. (1), where Π is the scalar self-energy, results in an overcounting of the two-loop figure-eight vacuum diagram on the left side of Eq. (2).[1] Shifting m^2 in the vacuum diagram is equivalent to dressing the propagator and three-point vertex of the one-loop tadpole, so this "full dressing" overcounts the two-loop figure-eight tadpole on the right side of Eq. (2) [4, 7]. We will show, by explicit calculation to 4 loops, that dressing only the propagator in a one-loop tadpole ("partial dressing") correctly counts the relevant graphs.

A. Dressing up

In both full and partial dressing procedures, the propagator is first improved by solving a gap equation:[2]

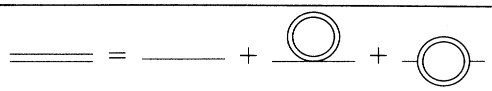

$$M^2 = m^2 - \tfrac{1}{2}c_4 I_1(M^2) - \tfrac{1}{2}c_3^2 I_2(M^2) \tag{3}$$

c_3 and c_4 are the 3- and 4-point vertices, respectively, with $dc_3/d\phi = c_4$. We have defined

$$\begin{aligned} I_0(m^2) &\equiv -T\sum_n \int \frac{d^3\mathbf{p}}{(2\pi)^3} \ln\left[(2\pi nT)^2 + p^2 + m^2\right], \\ I_j(m^2) &\equiv \ \ T\sum_n \int \frac{d^3\mathbf{p}}{(2\pi)^3} \left[(2\pi nT)^2 + p^2 + m^2\right]^{-j} \quad (j > 0). \end{aligned} \tag{4}$$

The dressed vertex is found by differentiating the mass gap equation and solving for the improved three-point function:

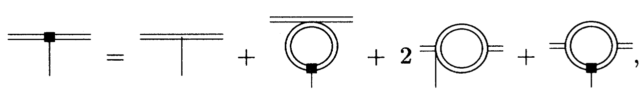 (5)

$$C_3 \equiv -\frac{dM^2}{d\phi} = c_3 + \tfrac{1}{2}C_3 c_4 I_2(M^2) + c_3 c_4 I_2(M^2) + C_3 c_3^2 I_3(M^2). \tag{6}$$

The prescription in [4] is to equate V' with a one-loop-improved propagator tadpole (partial dressing):

$V'_{\rm PD} =$ 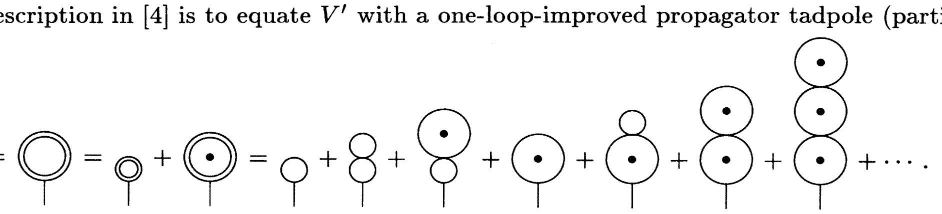 (7)

This contrasts with the procedure in [5], which consists of substituting M^2 into the one-loop potential $V = -\frac{1}{2}I_0(M^2)$, expanding and replacing M^2 by m^2 in all terms except the cubic M^3. Since the M^3 term arises precisely from the zero mode in the the one-loop tadpole, differentiating this expression by ϕ and expanding the vertex gives

$V'_{\rm FD} =$ 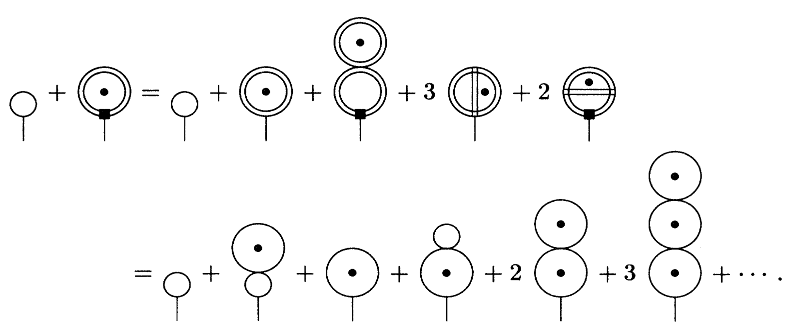 (8)

[1] In [5], when their equation (33) is substituted in (21) and expanded, the result for V includes a term $3\lambda T^2 m^2/32\pi^2$, which is twice the correct result.

[2] In all diagrammatic mass gap equations, we display only the one particle irreducible (1PI) diagrams from the usual infinite series.

A dot inside a loop means only zero modes are contained in that loop variable, although nonzero modes can run through shared propagators.

Although we have expanded the improved vertex and propagators graphically, the algebraic expansion is equally simple by repeated use of the recursion relation equation (6) and

$$\tfrac{c_3}{2}[I_1(M^2)] = \tfrac{c_3}{2}[I_1(m^2) + \tfrac{1}{2}c_4 I_2(m^2) I_1(M^2) + \tfrac{1}{4}c_4^2 I_1^2(M^2) I_3(m^2) + \tfrac{1}{8}c_4^3 I_1^3(M^2) I_4(m^2) + \cdots], \tag{9}$$

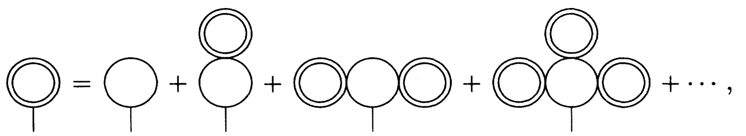

(10)

where the ellipsis refers to terms with powers of c_3 and higher powers of c_4. The result can then be compared to a Feynman graph computation of the one-point function to examine the validity of the two methods. In practice, gap equation solutions and loop integrals can only be approximated. However, as long as the same approximations are made in the Feynman diagram expansion, the results can still be consistently and explicitly compared.

B. Rules of the game

We now calculate the algebraic expressions and the Feynman diagrams for a real scalar theory, under some simplifying rules. All diagrams are preceded by an overall minus sign, to give V or its derivatives, and a symmetry factor. The vertices are $c_3 = -V_0''' = -6\lambda\phi$ and $c_4 = -V_0'''' = -6\lambda$. We ignore for now the ellipsis in Eq. (1); we will discuss the missing terms in Sec. III B. Temperature-dependent parts of loop integrals are then given by Table I (our combinatoric analysis will not hinge on zero temperature results, or on renormalization prescriptions). The leading-order result comes from a single hard (nonzero mode) thermal loop

$-\frac{1}{2}$ 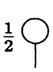 $= (6\lambda\phi)\dfrac{T^2}{24}.$ (11)

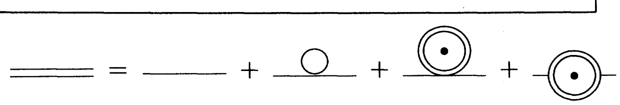

Note that in this approximation (which we will fix in Sec. III B), higher-loop diagrams made by attaching bubbles to this one vanish, due to the zeros in the first line of Table I.

Diagrams are categorized as being $O(\alpha^{j_\alpha}\beta^{j_\beta}\gamma^{j_\gamma})$ with respect to Eq. (11), where [5]

$$\alpha \equiv \lambda T^2/m^2 \approx 1, \quad \beta \equiv \lambda T/m < 1, \quad \gamma \equiv \phi^2/T^2 \ll 1, \tag{12}$$

in the region of interest to us. To keep things tractable (and minimize distractions from issues of overlapping momentum), we will first look only at $O(\gamma^0)$, meaning only one three-point vertex; higher orders are discussed in Sec. III. A scheme is called "accurate to $O(\beta^j)$" if it correctly reproduces all diagrams with $j_\beta \leq j$ and $j_\gamma = 0$.[3] In [4] we call $O(\beta)$ "daisy order," and $O(\beta^2)$ "superdaisy order." While the schemes described in this paper are not accurate to $O(\beta^3)$, we find it instructive here to analyze "daisy-type" graphs to $O(\beta^4)$. For illustrative purposes, we will display terms and diagrams only to $O(\lambda^4)$, which for $j_\gamma = 0$ means 4 loops.

C. Partial- and full-dressing results

To the order we are working, the gap equation is

$$M^2 = m^2 + \frac{\lambda T^2}{4} - \frac{3\lambda T M}{4\pi} - \frac{9\lambda^2\phi^2 T}{4\pi M}. \tag{13}$$

Although the last term is $O(\alpha\gamma)$ compared to the previous one, we retain it because their *derivatives* are the same order. We need not dress the nonzero-mode loop at this level of approximation, as discussed below Eq. (11).

The solution of the gap equation, expanded to $O(\lambda^3\gamma^0)$, is

$$M = m + \frac{\lambda T^2}{8m} - \frac{3\lambda T}{8\pi} - \frac{\lambda^2 T^4}{128 m^3} + \frac{9\lambda^2 T^2}{128\pi^2 m} + \frac{\lambda^3 T^6}{1024 m^5} - \frac{9\lambda^3 T^4}{1024\pi^2 m^3} + O(\lambda^4, \gamma^1) \tag{14}$$

TABLE I. Loop integrals.

Integral	I_0	I_1	I_2	I_3	I_4
Nonzero modes	$\left(\frac{\pi^2 T^4}{45} - \frac{T^2 m^2}{12}\right)$	$\frac{T^2}{12}$	0	0	0
Zero modes	$\frac{Tm^3}{6\pi}$	$\frac{-Tm}{4\pi}$	$\frac{T}{8\pi m}$	$\frac{T}{32\pi m^3}$	$\frac{T}{64\pi m^5}$

[3] In [5] diagrams are compared instead to the leading zero-mode loop, so their "$O(\bar{\beta})$" corresponds to our $O(\beta^2)$.

and the improved three-point coupling is

$$-\frac{dM^2}{d\phi} = -(6\lambda\phi)\left[1+\left\{-\frac{9\lambda T}{8\pi m}+\frac{9\lambda^2T^3}{64\pi m^3}-\frac{27\lambda^3T^5}{1024\pi m^5}+\frac{81\lambda^3T^3}{1024\pi^3m^3}\right\}+O(\lambda^4,\gamma^1)\right]. \tag{15}$$

Exactly 1/3 of the expression in curly brackets arises from the penultimate term in Eq. (13), and 2/3 from the last term, as can be seen by careful inspection of Eq. (5).

The partially dressed one-loop tadpole is then

$-\frac{1}{2}$ 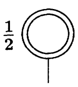 $= -\frac{1}{2}$ 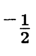 $+ (6\lambda\phi)\frac{-TM}{8\pi}$

$= -\frac{1}{2}$ 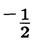 $+ (6\lambda\phi)$

$$\times\left[\frac{-Tm}{8\pi}-\frac{\lambda T^3}{64\pi m}+\frac{3\lambda T^2}{64\pi^2}+\frac{\lambda^2T^5}{1024\pi m^3}-\frac{9\lambda^2T^3}{1024\pi^3 m}-\frac{\lambda^3T^7}{8192\pi m^5}+\frac{9\lambda^3T^5}{8192\pi^3m^3}+O(\lambda^4,\gamma^1)\right], \tag{16}$$

where the leading piece was given in Eq. (11). The fully dressed one-loop tadpole is

$-\frac{1}{2}$  $+$ 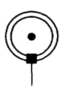 $= -\frac{1}{2}$ 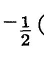 $+ \frac{dM^2}{d\phi}\frac{-TM}{8\pi}$

$= -\frac{1}{2}$ 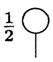 $+ (6\lambda\phi)$

$$\times\left[\frac{-Tm}{8\pi}-\frac{\lambda T^3}{64\pi m}+\frac{3\lambda T^2}{16\pi^2}+\frac{\lambda^2T^5}{1024\pi m^3}-\frac{63\lambda^2T^3}{1024\pi^3 m}-\frac{\lambda^3T^7}{8192\pi m^5}+\frac{63\lambda^3T^5}{8192\pi^3m^3}+O(\lambda^4,\gamma^1)\right]. \tag{17}$$

The difference is

$\Delta \equiv$ 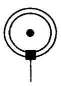 $-$ 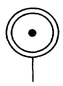

$$= (6\lambda\phi)\left[\frac{9\lambda T^2}{64\pi^2}-\frac{27\lambda^2T^3}{512\pi^3 m}+\frac{27\lambda^3T^5}{4096\pi^3m^3}+O(\lambda^4,\gamma^1)\right]. \tag{18}$$

The interpretation of Δ as a miscounting of graphs will become apparent after we compute the relevant Feynman diagrams.

Let us review the approximations implicit in the equations above. The hard figure-eight tadpole, Eq. (36), was lost when we dropped the ellipsis in Eq. (1); we will restore its $O(\beta^2)$ contribution in Sec. III B. We have (as did the authors of Refs. [5, 6]) ignored overlapping momenta in the last diagram of Eq. (13), introducing an error in Eq. (15) and thus in Eq. (17). With our judicious choice of $\gamma \ll 1$ we have avoided this error in Eqs. (14) and (16), but we will see in Sec. III C that overlapping momenta spoil our results, too, at $O(\gamma^1)$. None of these affect the counting arguments which are the main point of this section.

D. The diagrams

In addition to the leading result Eq. (11), the diagrams explicitly give

$-\frac{1}{2}$ 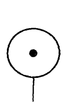 $= (6\lambda\phi)\frac{-Tm}{8\pi} \quad O(\alpha^{-1}\beta^1\gamma^0),$ (19)

$-\frac{1}{4}$ 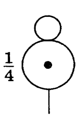 $= (6\lambda\phi)\frac{-\lambda T^3}{64\pi m} \quad O(\alpha^0\beta^1\gamma^0),$ (20)

$-\frac{1}{8}$ 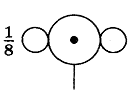 $= (6\lambda\phi)\frac{\lambda^2T^5}{1024\pi m^3} \quad O(\alpha^1\beta^1\gamma^0),$ (21)

$-\frac{1}{16}$ 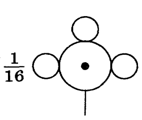 $= (6\lambda\phi)\frac{-\lambda^3T^7}{8192\pi m^5} \quad O(\alpha^2\beta^1\gamma^0),$ (22)

$-\frac{1}{4}$ 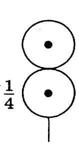 $= (6\lambda\phi)\frac{3\lambda T^2}{64\pi^2} \quad O(\alpha^{-1}\beta^2\gamma^0),$ (23)

$-\frac{1}{8}$ 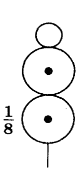 $+ -\frac{1}{4}$ 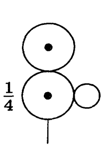 $= 0 \quad O(\alpha^0\beta^2\gamma^0),$ (24)

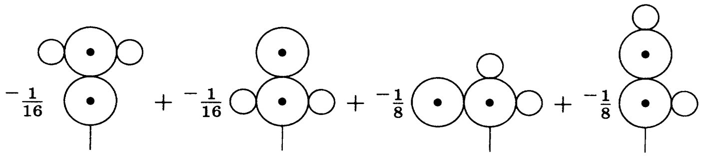

$$= 0 \quad O(\alpha^{1}\beta^{2}\gamma^{0}), \tag{25}$$

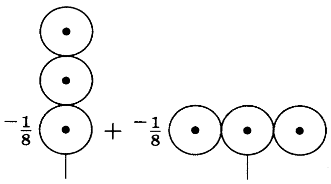

$$= (6\lambda\phi)\frac{-9\lambda^2T^3}{1024\pi^3 m} \quad O(\alpha^{-1}\beta^{3}\gamma^{0}), \tag{26}$$

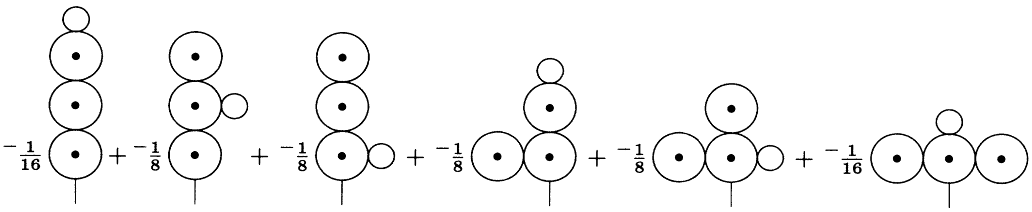

$$= (6\lambda\phi)\frac{9\lambda^3T^5}{8192\pi^3 m^3} \quad O(\alpha^{0}\beta^{3}\gamma^{0}), \tag{27}$$

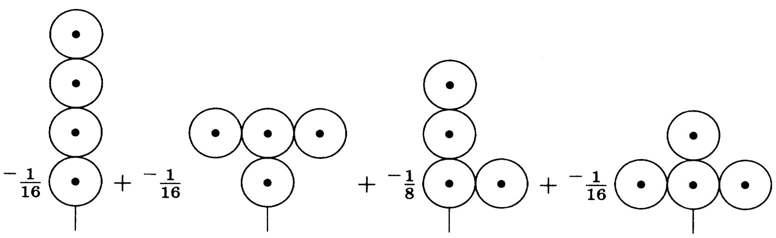

$$= 0 \quad O(\alpha^{-1}\beta^{4}\gamma^{0}). \tag{28}$$

Note that the order in β is the number of zero-mode loops, and the order in α is the number of nonzero-mode loops minus one.

A somewhat surprising result is that, except for the figure-eight daisy graph in Eq. (23), all $O(\beta^2)$ contributions sum to zero. That all $O(\beta^2)$ contributions from daisy and superdaisy diagrams cancel for any number of loops can be seen by schematically writing the solution to the quadratic gap equation [i.e., ignoring the last term in Eq. (13)] as

$$M \sim \beta^2 + \beta\sqrt{1+\beta^2}. \tag{29}$$

The first term of $O(\beta^2)$ corresponds to the subleading daisy graph of Eq. (23), which cannot cancel with a superdaisy because superdaisies first occur at three loops. Since all other terms in M are odd in β, the $O(\beta^2)$ contributions to the effective potential arising from zero modes (which at the tadpole level are proportional to M) must cancel. This remains true only while the trilinear coupling can be ignored. When they are included, M is the solution of a cubic equation containing both even and odd powers of β. This result has implications for the electroweak theory, where gauge boson gap equations can be approximated by a quadratic [4].[4]

Comparing the individual diagrams with the expansion equations (16) and (17) we see that the partially dressed tadpole gives precisely the correct results. Full dressing, Eq. (17), leads to 3 erroneous terms, starting at $O(\beta^2)$. Graphical and algebraic iteration of the gap equations show that one third of Δ in Eq. (18) arises from an overcounting of diagrams in Eqs. (23), (26), and (27) by two, three, and three, respectively. Full dressing overcounts the individual superdaisies and subleading daisies by a common factor, so that the sum still vanishes. However, this cancellation is no longer possible when trilinear couplings are reintroduced.

E. Lollipops

The other two-thirds of Δ arise from an attempt to include the lollipop (and its dressed cousins), which is

[4]Subsequent works have explored the electroweak gap equations in more detail [6, 13], and are in agreement with [4] up to, but not including, the ϕ-independent magnetic mass which is $\sim g^2T$. The effect of the magnetic mass term on the potential is $O(g^5)$ for $\phi \sim T$, and hence subleading in a consistent $O(\beta^2)$ calculation. However, at smaller values of ϕ the magnetic mass becomes increasingly important.

also superdaisy order [4, 8, 15]:

$-\frac{1}{6}$ 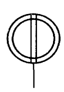 $$= (6\lambda\phi)\frac{\lambda T^2}{32\pi^2}\left[\ln\left(\frac{M^2}{T\bar{\mu}}\right) + 1.65\right] \qquad O(\alpha^{-1}\beta^2\gamma^0), \qquad (30)$$

where $\bar{\mu}$ is a renormalization scale, often taken to be T; and M is the improved mass of Eq. (14). The infrared behavior is calculable just from the zero modes. Recall that $m/T \sim \sqrt{\lambda}$, so for any reasonable Higgs boson mass the log term is near unity.

In the partial dressing method the lollipop is not considered a "daisy-type" diagram; the result Eq. (30) is just added to V'_{PD} to give $V'_{\mathrm{PD+L}}$.

The full-dressing method sees this diagram as an improved-propagator main loop attached to a vertex dressed with an improved-propagator bubble. Algebraically, it arises from

$$\tfrac{1}{2}\frac{\mathrm{d}M^2}{\mathrm{d}\phi}I_1(M^2) \ni \tfrac{1}{2}\left[c_3c_4I_2(M^2)\right] I_1(M^2). \qquad (31)$$

Symmetry factors of $\frac{1}{2}$ from the main loop and $\frac{1}{2}$ from the vertex loop combine with a factor of 2 ways to attach the external line to the four-point vertex, giving an overall factor of $\frac{1}{2}$ instead of the correct $\frac{1}{6}$. Overlapping momenta and nonzero modes are ignored. Then

$$-\tfrac{1}{2}(-6\lambda\phi)(-6\lambda)\left(\frac{-Tm}{4\pi}\right)\left(\frac{T}{8\pi m}\right) = (6\lambda\phi)\frac{3\lambda T^2}{32\pi^2} \qquad (32)$$

which is the leading term of $\frac{2}{3}\Delta$. Because overlapping momenta are ignored, the logs of the true calculation are not reproduced. In principle, using the momentum-dependent self-energy in the gap equations would result in inclusion of the logs, but the combinatoric miscounting would remain.

The leading term of $V'_{\mathrm{FD}} - V'_{\mathrm{PD+L}}$ (i.e., the error in the full-dressing calculation) arises from one extra figure-eight tadpole [Eq. (23)] and two extra lollipops [2/3 of Eq. (32) in the approximation that overlapping momenta are ignored]; these are then subtracted off with

$$V'_{\mathrm{comb}} = (6\lambda\phi)\frac{-7\lambda T^2}{64\pi^2} \qquad (33)$$

as given in [6] (but apparently neglected in [5]). At each order in β more terms of V'_{comb} would need to be calculated to correct the full-dressing method, since [as we saw in Eqs. (8) and (18)] full dressing overcounts an infinite class of diagrams. The Cornwall-Jackiw-Tomboulis (CJT) technique we will discuss in Sec. IV provides a systematic, if cumbersome, way to calculate V'_{comb}.

III. TYING UP LOOSE ENDS

Many approximations were made in the previous section in order to facilitate an explicit counting of diagrams. Here we will reexamine them and develop a general $O(\beta^2)$ procedure for calculating $V'_{\mathrm{PD+L}}$.

A. Nondaisies

Diagrams besides the "daisy-type" ones and the lollipops are all either higher-order in γ or at least $O(\beta^3)$, e.g.,

$-\frac{1}{12}$ 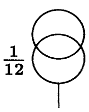 $$\sim (6\lambda\phi)\frac{3\lambda^2 T^3}{128\pi^3 m}\ln(T/m) \quad O(\alpha^{-1}\beta^3\gamma^0). \qquad (34)$$

(The infrared behavior was calculated from zero modes as for the lollipop.) There would be little point deriving a potential accurate to $O(\beta^3)$ unless these diagrams were also included.

B. Log terms and dressed nonzero-mode loops

By ignoring the ellipsis in Eq. (1) we not only reduced the number of diagrams to calculate, but also evaded the question of whether to dress nonzero-mode loops. In Table II we now restore terms proportional to $L \equiv \ln(\bar{\mu}^2/T^2) - 2c_B$, where $2c_B = 2\ln(4\pi) - 2\gamma_E \approx 3.9076$ and $\bar{\mu}$ is a renormalization scale. When determining the order of a diagram we will treat L as order 1.

The diagrams of Eqs. (19)–(28) now have subleading pieces, and new diagrams (with nonzero-mode loops of several propagators) appear. We will spare the reader by mentioning just the two new $O(\beta^2)$ contributions:

$-\frac{1}{2}$ 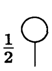 $$[\text{subleading}] = (6\lambda\phi)\frac{-m^2L}{32\pi^2} \quad O(\alpha^{-2}\beta^2\gamma^0), \qquad (35)$$

$-\frac{1}{4}$ 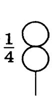 $$= (6\lambda\phi)\frac{-\lambda T^2 L}{128\pi^2} \quad O(\alpha^{-1}\beta^2\gamma^0). \qquad (36)$$

These (and higher-order generalizations) can be accounted for by keeping the L term in the one-loop tadpole, Eq. (11), and using the improved mass M in the $\frac{m}{T}$ expansion. This corresponds to improving both zero- and nonzero-mode propagators as done in [4]. The full-dressing method of Refs. [5, 6] improves only zero modes, and therefore omits the $O(\beta^2)$ graph in Eq. (36).

TABLE II. Rules including log term $L \equiv \ln(\bar{\mu}^2/T^2) - 3.9076$.

Integral	I_0	I_1	I_2	I_3
Nonzero modes	$\left(\frac{\pi^2T^4}{45} - \frac{T^2m^2}{12} + \frac{m^4L}{32\pi^2}\right)$	$\left(\frac{T^2}{12} - \frac{m^2L}{16\pi^2}\right)$	$\frac{L}{16\pi^2}$	0
Zero modes	$\frac{Tm^3}{6\pi}$	$\frac{-Tm}{4\pi}$	$\frac{T}{8\pi m}$	$\frac{T}{32\pi m^3}$

C. Three-point vertices

Let us now examine $O(\gamma^1)$ diagrams containing three three-point vertices and up to 3 loops. When $\lambda\phi^2$ terms are retained in the gap equation Eq. (13), results Eqs. (16) and (17) are modified to

$-\frac{1}{2}$ 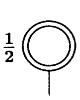 $$= (6\lambda\phi)\left[(\text{old}) + \frac{9\lambda^2\phi^2T^2}{64\pi^2m^2} - \frac{9\lambda^3\phi^2T^4}{256\pi^2m^4} + \frac{27\lambda^3\phi^2T^3}{512\pi^3m^3} + O(\lambda^4,\gamma^2)\right], \quad (37)$$

$-\frac{1}{2}$ 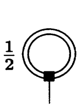 $$= (6\lambda\phi)\left[(\text{old}) + \frac{81\lambda^3\phi^2T^3}{512\pi^3m^3} + O(\lambda^4,\gamma^2)\right]. \quad (38)$$

The new two-loop diagram is the "setting sun" tadpole

$-\frac{1}{4}$ 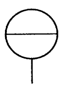 $$= (6\lambda\phi)\frac{6\lambda^2\phi^2T^2}{64\pi^2m^2}\ (\text{true}) \approx (6\lambda\phi)\frac{9\lambda^2\phi^2T^2}{64\pi^2m^2}\ (\text{naive}) \quad O(\alpha^0\beta^2\gamma^1). \quad (39)$$

The "true" result is from the double integral done properly; the "naive" result comes from ignoring the overlapping momenta and using Table I, assigning two propagators to each of the integrals. This is the approximation that has been criticized in [8], and amounts to approximating a momentum-dependent self-energy $\Pi(Q^2)$ by its zero momentum value $\Pi(0)$. The naive result is 3/2 times the true result, which as suggested in [8] is a significant error. This error is exacerbated in the electroweak theory, where logarithms from analogous diagrams are lost if $\Pi(0)$ is used. Here, we are interested in counting arguments which are independent of whether one uses $\Pi(0)$ or $\Pi(Q^2)$.

Note that partial dressing of the one-loop tadpole [Eq. (37)] correctly reproduces the "naive" result, while full dressing [Eq. (38)] does not. More subtly, full dressing counts the setting sun tadpole once as a dressed propagator and twice as a dressed vertex, which happen to cancel (because overlapping momenta are treated differently) and give zero. If $\Pi(Q^2)$ were used, the diagrams would instead add, leading to a miscount of three.[5]

At 3 loops we have

$-\frac{1}{4}$ 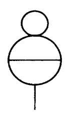 $+\ -\frac{1}{4}$ 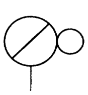 $$= (6\lambda\phi)\frac{-6\lambda^3\phi^2T^4}{256\pi^2m^4}\ (\text{true}), \quad \approx (6\lambda\phi)\frac{-9\lambda^3\phi^2T^4}{256\pi^2m^4}\ (\text{naive}) \quad O(\alpha^1\beta^2\gamma^1), \quad (40)$$

$-\frac{1}{4}$ 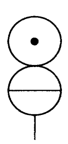 $+\ -\frac{1}{4}$ 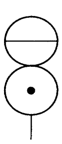 $+\ -\frac{1}{4}$ 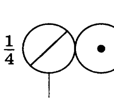 $$= (6\lambda\phi)\frac{18\lambda^3\phi^2T^3}{512\pi^3m^3}\ (\text{true}) \quad \approx (6\lambda\phi)\frac{27\lambda^3\phi^2T^3}{512\pi^3m^3}\ (\text{naive}) \quad O(\alpha^0\beta^3\gamma^1). \quad (41)$$

We see again that partial dressing correctly counts the naive calculations of these graphs. Since the naive results are again 3/2 times the true results (hard loop dressings do not affect momentum flow), we can multiply the last term in the gap equation (13) by 2/3 to correct for using $\Pi(0)$ instead of $\Pi(Q^2)$. This is just a simple way to implement our explicit calculations, and does not represent a systematic improvement of the partial dressing method.

We can show that no tadpole graphs with $j_\gamma > 1$ contribute at $O(\beta^2)$. Roughly, every additional factor of γ means two more three-point vertices, which form either a zero-mode loop (contributing β) or a two-propagator nonzero-mode loop (contributing β^2). More precisely, a graph with Z zero-mode loops, N_1 one-propagator nonzero-mode loops, N_2 two-propagator nonzero-mode loops, f four-point vertices, and t three-point vertices, obeys

$$f + \tfrac{1}{2}(t+1) = Z + N_1 + N_2, \quad j_\alpha - j_\gamma + 1 = N_1 - N_2,$$
$$j_\beta = Z + 2N_2, \quad j_\gamma = \tfrac{1}{2}(t-1). \quad (42)$$

Except for the leading diagram equation (11), $f \geq N_1$, from which it follows that

$$j_\beta \geq (Z + N_2) \geq \tfrac{1}{2}(t+1) = j_\gamma + 1. \quad (43)$$

D. The full result of partial dressing

To summarize, our results, good to $O(\beta^2)$ (and all orders in α and γ), are

[5] In the electroweak calculation of [6], the gauge boson analogue of the figure-eight graph equation (23) was subtracted once, and the gauge boson analogue of the setting sun graph equation (39) was subtracted twice by a term $V_{\rm comb}$, correctly compensating for the miscounting of these diagrams. However, topologically equivalent diagrams outside the pure gauge sector remain overcounted (for example, the setting sun vacuum graph consisting of one Higgs boson and two gauge boson propagators).

$V'_{\mathrm{PD+L}} = {}^{-\frac{1}{2}}$ 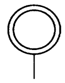 $+ {}^{-\frac{1}{6}}$ 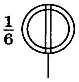

$$= (6\lambda\phi)\left[\frac{T^2}{24} - \frac{TM}{8\pi} - \frac{M^2L}{32\pi^2} + \frac{\lambda T^2}{32\pi^2}\left\{\ln\left(\frac{M^2}{T\bar{\mu}}\right) + 1.65\right\}\right], \quad (44)$$

$$M^2 = m^2 + \frac{\lambda T^2}{4} - \frac{3\lambda TM}{4\pi} - \frac{2}{3}\frac{9\lambda^2\phi^2 T}{4\pi M},$$

$$L \equiv \ln(\bar{\mu}^2/T^2) - 3.9076.$$

Here the "true" results of Eq. (39), etc., have been incorporated by the new factor of 2/3 in the gap equation. Note that despite the resummation of nonzero modes, no linear term has been generated, since $V'_{\mathrm{PD+L}}(\phi = 0) = 0$.

IV. OTHER METHODS

A. The CJT technique

Amelino-Camelia and Pi [11] employ the technique of Cornwall, Jackiw, and Tomboulis (CJT) [12] to derive an effective action

$$\Gamma[\phi] = I_{\mathrm{cl}}[\phi] + \Gamma^{(1)}[\phi, G] + \Gamma^{(2)}[\phi, G] - \mathrm{Tr}\left\{\frac{\delta\Gamma^{(2)}[\phi, G]}{\delta G} G\right\}, \quad (45)$$

where $\Gamma^{(1)}$ is the improved one-loop vacuum graph, $\Gamma^{(2)}$ consists of 2PI graphs with improved propagators and unimproved vertices, and the improved propagator G comes from a gap equation

$$G^{-1} = D^{-1} + 2\frac{\delta\Gamma^{(2)}[\phi, G]}{\delta G}. \quad (46)$$

Roughly translated, Eq. (45) says that any n-propagator diagram arising from the fully dressed one-loop vacuum graph must be subtracted off $(n-1)$ times.

Suppose we put only the (two-propagator) figure-eight vacuum graph of Eq. (2) into $\Gamma^{(2)}$ (as done in [11]). The gap equation becomes

 $\quad \bar{M}^2 = m^2 - \frac{1}{2}c_4 I_1(\bar{M}^2) \quad (47)$

and the tadpole equivalent of Eq. (45) is

$V'_{\mathrm{CJT1}} = {}^{-\frac{1}{2}}$ 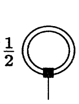 $- {}^{-\frac{1}{4}}$ 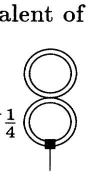

$$= {}^{-\frac{1}{2}}C_3\, I_1(\bar{M}^2) + \tfrac{1}{4}C_3 c_4\, I_1(\bar{M}^2) I_2(\bar{M}^2). \quad (48)$$

But the gap equation implies the identity

$$C_3[1 - \tfrac{1}{2}c_4 I_2(\bar{M}^2)] = c_3 \quad (49)$$

so

$V'_{\mathrm{CJT1}} = {}^{-\frac{1}{2}}c_3\, I_1(\bar{M}^2) = {}^{-\frac{1}{2}}$ 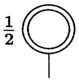 $= V'_{\mathrm{PD}}. \quad (50)$

The CJT procedure with this $\Gamma^{(2)}$ gives precisely the same result as the partially dressed tadpole of Eq. (16), in the limit $\gamma \ll 1$. We have already noted that the lollipop is leading order in γ and must be added by hand to V'_{PD}, so the same applies to this version of CJT.

Now let us also include the (three-propagator) two-loop "setting sun" diagram in $\Gamma^{(2)}$. The gap equation is Eq. (3), and

$V'_{\mathrm{CJT2}} = {}^{-\frac{1}{2}}$ 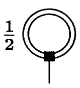 $- {}^{-\frac{1}{4}}$ 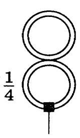 $-2\ {}^{-\frac{1}{6}}$ 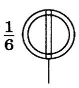 $-2\ {}^{-\frac{1}{4}}$ 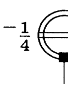 . $\quad (51)$

The gap equation now implies the identity

$$C_3[1 - \tfrac{1}{2}c_4 I_2(M^2) - c_3^2 I_3(M^2)] = c_3 + c_3 c_4 I_2(M^2) \quad (52)$$

so that (ignoring overlapping momentum)

$V'_{\mathrm{CJT2}} = {}^{-\frac{1}{2}}$ 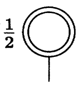 $+ {}^{-\frac{1}{6}}$ 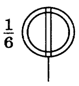 $= V'_{\mathrm{PD+L}}. \quad (53)$

The partially dressed tadpole (for general γ) plus lollipop, Eq. (44), has now been recovered. We again see in Eq. (51) that full dressing overcounts 1 extra figure-eight, 2 extra lollipops, and 2 extra setting-suns; the CJT technique provides a systematic way of calculating V'_{comb}.

When done more carefully, the CJT technique may be capable of handling overlapping momenta, but we are unaware of any such analysis.

B. Restoring the loop expansion

Arnold and Espinosa [8] suggest another method of resumming daisies which restores the loop expansion. They note that each zero-mode loop costs at least a factor of β, so to compute to $O(\beta^2)$, one need evaluate only graphs with two or fewer zero-mode loops. This avoids any combinatoric complications due to field-dependent mass shifts. Hard thermal loops on zero-mode propagators are resummed by shifting the mass with a temperature-dependent but field-independent quantity,

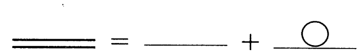 $\quad \bar{m}^2 = m^2 + \frac{\lambda T^2}{4} \quad (54)$

so $m \to \bar{m}$ only in the bottom row of Table II. A "thermal counterterm" is introduced to cancel the overcounting of graphs which occurs when improved propagators are used in a loop expansion [15]:

 $= \frac{\lambda T^2}{4}. \quad (55)$

The counterterm ensures that the one-point function result remains unchanged even if nonzero modes are also resummed. Then

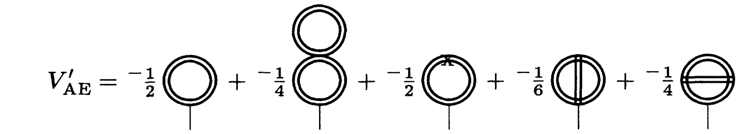

$$= (6\lambda\phi)\left[\frac{T^2}{24} - \frac{T\bar{m}}{8\pi} - \frac{m^2 L}{32\pi^2} - \frac{\lambda T^2 (L-6)}{128\pi^2} + \frac{\lambda T^2}{32\pi^2}\left\{\ln\left(\frac{\bar{m}^2}{T\bar{\mu}}\right) + 1.65\right\} + \frac{6\lambda^2\phi^2 T^2}{64\pi^2 \bar{m}^2}\right] \qquad (56)$$

which agrees with Eq. (44) to $O(\beta^2)$.

The result for diagram counting is identical to partial dressing. However, because the two loop graphs are being explicitly evaluated, overlapping momentum are always handled correctly. This is a significant improvement over the partial dressing method.

Another advantage to this zero-mode loop expansion is that it easily generalizes to higher order in β. One must be careful, however, if it becomes necessary to shift the mass in a field dependent way. In the Abelian Higgs model, a cancellation [8] eliminates the need to do this at $O(\beta^2)$. It is not clear to us if this will be true at $O(\beta^3)$. If not, it is important to partially dress rather than to simply insert the improved mass into the one-loop vacuum graph.

C. The two-point way

Near the completion of our work, we became aware of another treatment of the electroweak phase transition by Buchmuller, Fodor, Helbig, and Walliser [13]. These authors solve gap equations for scalar and vector boson propagators (two-point functions), and integrate (effectively, twice) to get the effective potential. As they point out, the result contains all of the $O(\beta)$ corrections, but only some of the $O(\beta^2)$ corrections. Applied to scalar ϕ^4 theory, we believe their procedure is equivalent to integrating our gap equation (3) twice. This differs from the partial dressing method, which inserts the solution of the gap equation into a one-loop tadpole, going one iteration further in the improvement of the effective potential.

By differentiating Eq. (44) and using Eq. (5), we see that our $O(\beta^2)$, partial-dressing improved mass squared is

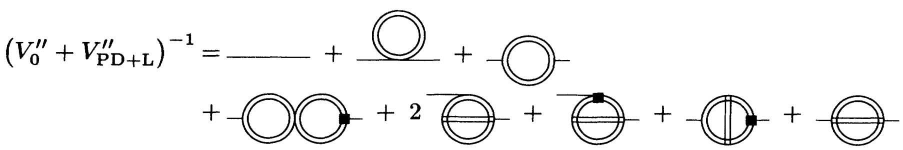

(57)

which contrasts sharply with the M^2 of Eq. (3); to be precise, the two-point method of [13] misses all the two-loop 1PI diagrams of Eq. (57). In addition, it suffers the usual problems with overlapping momenta.

D. The hybrid way

We have seen that partial dressing makes correct counting easy, but overlapping momenta [in the last term of the gap equation Eq. (13)] are problematic. We now propose using the gap equation of Eq. (47), which dresses the propagator with only momentum-independent loops, and calculating the setting sun vacuum graph (which gives both the setting sun tadpole and the lollipop) separately, with only hard thermal loop dressings, as done by Arnold and Espinosa. Then we get a potential correct to $O(\beta^2)$ from only two graphs (and one quadratic gap equation):

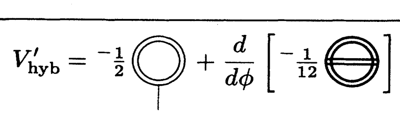

(58)

$$=(6\lambda\phi)\left[\frac{T^2}{24} - \frac{T\bar{M}}{8\pi} - \frac{\bar{M}^2 L}{32\pi^2}\right] + \frac{d}{d\phi}\left[\frac{3\lambda^2\phi^2 T^2}{32\pi^2}\left\{\ln\left(\frac{\bar{m}^2}{T\bar{\mu}}\right) + 1.65\right\}\right],$$

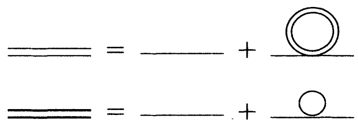

$$\bar{M}^2 = m^2 + \frac{\lambda T^2}{4} - \frac{3\lambda T\bar{M}}{4\pi},$$

$$\bar{m}^2 = m^2 + \frac{\lambda T^2}{4},$$

and again $L \equiv \ln(\bar{\mu}^2/T^2) - 3.9076$. This hybrid method generalizes easily to $O(\beta^3)$ just by adding all three-loop vacuum graphs with overlapping momenta, and should be just as applicable to more complicated theories such as the standard model. We expect the computational utility of the hybrid method to be more apparent in such generalizations.

V. CONCLUSION: WHAT'S HOT AND WHAT'S NOT

A. Summary of results

We have examined various prescriptions for calculating $O(\beta^2)$ contributions to the effective potential in a scalar ϕ^4 theory, by comparing the first few terms in a loop expansion to explicit Feynman graph computations.

We showed that fully dressed tadpoles (or equivalently, dressed vacuum diagrams) overcount an infinite class of diagrams, overcount and incorrectly calculate lollipop-type diagrams, miss significant contributions arising from nonzero modes, and suffer corrections (even for $\gamma \ll 1$) due to overlapping momenta [approximating $\Pi(Q^2) \approx \Pi(0)$]. In order to calculate V' to $O(\beta^2)$ correctly, one needs to subtract the overcounted figure-eight tadpole and lollipop (i.e., include $V'_{\rm comb}$), compensate for overlapping momentum corrections (in the lollipop), restore the hard-loop dressed setting sun tadpole, and include the hard figure-eight of Eq. (36).

Partially dressed tadpoles completely miss lollipop-type diagrams, and suffer overlapping momentum corrections. In order to calculate V' to $O(\beta^2)$ correctly, one needs to add the lollipop by hand (as done in [4]), and compensate for momentum corrections in the hard-loop dressed setting sun tadpole [as seen in Eq. (39)]. The prescription for scalar ϕ^4 theory is given in Eq. (44).

The CJT method, Eq. (45), provides a systematic way of removing the overcounted diagrams of the full dressing method, but we do not know how to extend it to correctly calculate overlapping momenta. As it stands now, it is equivalent to partial dressing.

The hard-loop dressing of Arnold and Espinosa, Eq. (56), counts diagrams correctly (through the use of "thermal counterterms"), and no overlapping momentum errors are incurred because all such diagrams are calculated explicitly. This task is somewhat easier if one sticks to vacuum graphs.

The two-point method of Buchmuller *et al.* [13] does not seem to be an attempt at a complete $O(\beta^2)$ calculation.

Finally, we suggested in Eq. (58) a simple synthesis of the above procedures. A tadpole is partially dressed with only momentum-independent loops (both zero and nonzero modes), and all other diagrams are calculated by hand at the vacuum level, using hard-loop dressing. At $O(\beta^2)$ there is only one such diagram, the setting sun.

B. Outlook for the EWPT

Although the analysis presented here is in the context of scalar ϕ^4 theory, the conclusions are equally valid for the electroweak phase transition (the main difference being an exacerbation of errors due to new graphs involving gauge bosons). This allows us to examine recent conflicting claims about the nature of the EWPT.

In a previous paper [4], the authors, using partial dressing, found $O(\beta^2)$ contributions to the effective potential which weakened the phase transition. The transition remained first order over the range of validity of our calculation. We estimated the effects of ignoring overlapping momentum, suggesting it would be numerically small. It has since been shown that this $O(\beta^2)$ contribution is logarithmically enhanced [8, 9], so that the partial dressing method in [4] is incomplete. In particular, setting sun-type diagrams need to be handled more carefully to produce an effective potential reliable to $O(\beta^2)$.

Espinosa, Quiros, and Zwirner [6], using full dressing with a $V_{\rm comb}$ correction, find a weakened EWPT which becomes second order near the limits of their range of validity. They also ignore overlapping momenta. In addition, their $V_{\rm comb}$ neglects some overcounted graphs in the Higgs-gauge sector, and they ignore $O(\beta^2)$ contributions arising from nonzero-mode figure-eight graphs. For these reasons, their results are not reliable to $O(\beta^2)$.

A more strongly first order EWPT has been reported by Arnold and Espinosa [8]. We have seen that for ϕ^4 theory, their counting agrees with partial dressing, and their method handles overlapping momenta correctly, so we believe this result is reliable. We have verified their explicit computations only for the scalar ϕ^4 theory. This method seems easily generalizable to higher order in β, though any such generalization must take care to count graphs correctly if diagrams are resummed in a field-dependent manner. We expect the hybrid method of Eq. (58) applied to the EWPT would give results similar to those of Arnold and Espinosa.

ACKNOWLEDGMENTS

We thank Peter Arnold, Stamatis Vokos, Jose Ramon Espinosa, Mariano Quiros, and Fabio Zwirner for their patient and helpful discussions. C.G.B. acknowledges support from the National Science Foundation under Grant No. NSF-PHY-91-23780 and the U.S. Department of Energy under Grant No. DEFG-02-90ER40560. D.E.B. acknowledges support from the U.S. Department of Energy under Grant No. DE-FG03-92-ER40701. S.D.H. acknowledges support from the National Science Foundation under Grant No. NSF-PHY-92-18167, the state of Texas under Grant No. TNRLC-RGFY9106, the Milton Fund of the Harvard Medical School and from the Harvard Society of Fellows.

[1] D. Kirzhnits and A. Linde, Ann. Phys. (N.Y.) **101**, 195 (1976).
[2] D.E. Brahm and S.D.H. Hsu, Report No. CALT-68-1705 / HUTP-91-A063, 1991 (unpublished).
[3] M.E. Carrington, Phys. Rev. D **45**, 2933 (1992).
[4] C.G. Boyd, D.E. Brahm, and S.D.H. Hsu, preceding paper, Phys. Rev. D **48**, 4952 (1993).
[5] J.R. Espinosa, M. Quiros, and F. Zwirner, Phys Lett. B **291**, 115 (1992).
[6] J.R. Espinosa, M. Quiros, and F. Zwirner, Phys. Lett. B **314**, 206 (1993).
[7] M. Dine, R.G. Leigh, P. Huet, A. Linde, and D. Linde,

Phys. Lett. B **283**, 319 (1992); Phys. Rev. D **46**, 550 (1992).
[8] P. Arnold, Phys. Rev. D **46**, 2628 (1992); P. Arnold and O. Espinosa, *ibid.* **47**, 3546 (1993).
[9] J.E. Bagnasco and M. Dine, Phys. Lett. B **303**, 308 (1993).
[10] L. Dolan and R. Jackiw, Phys. Rev. D **9**, 3320 (1974).
[11] G. Amelino-Camelia and S.-Y. Pi, Phys. Rev. D **47**, 2356 (1993).
[12] J.M. Cornwall, R. Jackiw, and E. Tomboulis, Phys. Rev. D **10**, 2428 (1974).
[13] W. Buchmuller, Z. Fodor, T. Helbig, and D. Walliser, Report No. DESY 93-021, 1993 (unpublished).
[14] S.Y. Lee and A.M. Sciaccaluga, Nucl. Phys. **B96**, 435 (1975).
[15] R.R. Parwani, Phys. Rev. D **45**, 4695 (1992).